

# Flavor content of nucleon form factors in a VMD approach

R. Bijker

Instituto de Ciencias Nucleares, Universidad Nacional Autónoma de México, AP 70-543, 04510 México DF, México

Received: date / Revised version: date

**Abstract.** The strange form factors of the nucleon are studied in a two-component model consisting of a three-quark intrinsic structure surrounded by a meson cloud. A comparison with the available experimental world data from the SAMPLE, PVA4, HAPPEX and G0 collaborations shows a good overall agreement. It is shown that the strangeness contribution to the electric and magnetic form factors is of the order of a few percent. In particular, the strange quark contribution to the charge radius is small  $\langle r_s^2 \rangle_E = 0.005 \text{ fm}^2$  and to the magnetic moment it is positive  $\mu_s = 0.315 \mu_N$ .

**PACS.** 13.40.Gp Electromagnetic form factors – 12.40.Vv Vector-meson dominance – 14.20.Dh Protons and neutrons – 13.40.Em Electric and magnetic moments

## 1 Introduction

The flavor content of the electromagnetic form factors of the nucleon can be studied by combining the nucleon's response to the electromagnetic and weak neutral vector currents [1]. In recent experiments, parity-violating elastic electron-proton scattering has been used to probe the contribution of strange quarks to the structure of the nucleon [2,3]. The strange quark content of the form factors can be determined assuming charge symmetry and combining parity-violating asymmetries with measurements of the electric and magnetic form factors of the proton and neutron. The study of the strange quark content is of special interest because it is exclusively part of the quark-antiquark sea.

The experimental results from the SAMPLE, PVA4, HAPPEX and G0 collaborations have shown evidence for a nonvanishing strange quark contribution to the structure of the nucleon. In particular, evidence was found that the strange magnetic moment of the proton is positive [4], suggesting that the strange quarks reduce the proton's magnetic moment. This is an unexpected and surprising finding, since a majority of theoretical studies favors a negative value [5].

The aim of this contribution is to study the flavor content of nucleon form factors in a VMD approach in which the two-component model of electromagnetic nucleon form factors of [6] is extended to the strange sector. The strangeness content is determined via the coupling of the strange current to the  $\phi$  and  $\omega$  mesons [7]. A comparison with the available experimental world data shows a good overall agreement for  $0 < Q^2 < 1 \text{ (GeV/c)}^2$ .

## 2 Nucleon form factors

Electromagnetic and weak form factors contain the information about the distribution of electric charge and magnetization inside the nucleon. These form factors arise from matrix elements of the corresponding vector current operators

$$\langle N | V_\mu | N \rangle = \bar{u}_N \left[ F_1(Q^2) \gamma_\mu + F_2(Q^2) \frac{i\sigma_{\mu\nu} q^\nu}{2M_N} \right] u_N. \quad (1)$$

Here  $F_1$  and  $F_2$  are the Dirac and Pauli form factors which are functions of the squared momentum transfer  $Q^2 = -q^2$ . The electric and magnetic form factors,  $G_E$  and  $G_M$ , are obtained from  $F_1$  and  $F_2$  by the relations  $G_E = F_1 - \tau F_2$  and  $G_M = F_1 + F_2$  with  $\tau = Q^2/4M_N^2$ .

The Dirac and Pauli form factors are parametrized according to a two-component model of the nucleon [6] in which the external photon couples both to an intrinsic three-quark structure described by the form factor  $g(Q^2)$  and to a meson cloud through the intermediate vector mesons  $\rho$ ,  $\omega$  and  $\phi$ . In the original version of the two-component model [8], the Dirac form factor was attributed to both the intrinsic structure and the meson cloud, and the Pauli form factor entirely to the meson cloud. In a modified version [6], it was shown that the addition of an intrinsic part to the isovector Pauli form factor as suggested by studies of relativistic constituent quark models in the light-front approach [9], improves the results for the electromagnetic form factors of the neutron considerably.

In order to incorporate the contribution of the isoscalar ( $\omega$  and  $\phi$ ) and isovector ( $\rho$ ) vector mesons, it is convenient to first introduce the isoscalar and isovector current operators

$$V_\mu^{I=0} = \frac{1}{6} (\bar{u}\gamma_\mu u + \bar{d}\gamma_\mu d - 2\bar{s}\gamma_\mu s),$$

$$V_\mu^{I=I} = \frac{1}{2} (\bar{u}\gamma_\mu u - \bar{d}\gamma_\mu d). \quad (2)$$

The corresponding isoscalar Dirac and Pauli form factors depend on the couplings to the  $\omega$  and  $\phi$  mesons

$$F_1^{I=0}(Q^2) = \frac{1}{2}g(Q^2) [1 - \beta_\omega - \beta_\phi + \beta_\omega \frac{m_\omega^2}{m_\omega^2 + Q^2} + \beta_\phi \frac{m_\phi^2}{m_\phi^2 + Q^2}], \quad (3)$$

$$F_2^{I=0}(Q^2) = \frac{1}{2}g(Q^2) \left[ \alpha_\omega \frac{m_\omega^2}{m_\omega^2 + Q^2} + \alpha_\phi \frac{m_\phi^2}{m_\phi^2 + Q^2} \right],$$

and the isovector ones on the coupling to the  $\rho$  meson [6]

$$F_1^{I=1}(Q^2) = \frac{1}{2}g(Q^2) \left[ 1 - \beta_\rho + \beta_\rho \frac{m_\rho^2}{m_\rho^2 + Q^2} \right],$$

$$F_2^{I=1}(Q^2) = \frac{1}{2}g(Q^2) \left[ \frac{\mu_p - \mu_n - 1 - \alpha_\rho}{1 + \gamma Q^2} + \alpha_\rho \frac{m_\rho^2}{m_\rho^2 + Q^2} \right]. \quad (4)$$

The proton and neutron form factors correspond to the sum and difference of the isoscalar and isovector contributions,  $F_i^p = F_i^{I=0} + F_i^{I=1}$  and  $F_i^n = F_i^{I=0} - F_i^{I=1}$ , respectively. This parametrization ensures that the three-quark contribution to the anomalous magnetic moment is purely isovector, as given by  $SU(6)$ . The intrinsic form factor is a dipole  $g(Q^2) = (1 + \gamma Q^2)^{-2}$  which coincides with the form used in an algebraic treatment of the intrinsic three-quark structure [10]. The large width of the  $\rho$  meson which is crucial for the small  $Q^2$  behavior of the form factors, is taken into account in the same way as in [6,8]. For small values of  $Q^2$  the form factors are dominated by the meson dynamics, whereas for large values they satisfy the asymptotic behavior of p-QCD,  $F_1 \sim 1/Q^4$  and  $F_2 \sim 1/Q^6$  [11].

### 3 Flavor content

The strange quark content of the nucleon form factors arises through the coupling of the strange current

$$V_\mu^s = \bar{s}\gamma_\mu s, \quad (5)$$

to the intermediate isoscalar vector mesons  $\omega$  and  $\phi$  (using the convention of Jaffe [7]). The wave functions of the  $\omega$  and  $\phi$  mesons are given by

$$|\omega\rangle = \cos \epsilon |\omega_0\rangle - \sin \epsilon |\phi_0\rangle, \\ |\phi\rangle = \sin \epsilon |\omega_0\rangle + \cos \epsilon |\phi_0\rangle, \quad (6)$$

where the mixing angle  $\epsilon$  represents the deviation from the ideally mixed states  $|\omega_0\rangle = (u\bar{u} + d\bar{d})/\sqrt{2}$  and  $|\phi_0\rangle = s\bar{s}$ . Under the assumption that the strange form factors have the same form as the isoscalar ones, the Dirac and Pauli form factors that correspond to the strange current are

expressed as the product of an intrinsic part  $g(Q^2)$  and a contribution from the vector mesons

$$F_1^s(Q^2) = \frac{1}{2}g(Q^2) \left[ \beta_\omega^s \frac{m_\omega^2}{m_\omega^2 + Q^2} + \beta_\phi^s \frac{m_\phi^2}{m_\phi^2 + Q^2} \right],$$

$$F_2^s(Q^2) = \frac{1}{2}g(Q^2) \left[ \alpha_\omega^s \frac{m_\omega^2}{m_\omega^2 + Q^2} + \alpha_\phi^s \frac{m_\phi^2}{m_\phi^2 + Q^2} \right]. \quad (7)$$

The isoscalar and strange couplings appearing in Eqs. (4) and (7) are not independent of one another, but depend on the same nucleon-meson and current-meson couplings [7]. In addition, they are constrained by the electric charges and magnetic moments of the nucleon which leads to two independent isoscalar couplings

$$\alpha_\omega = \mu_p + \mu_n - 1 - \alpha_\phi, \\ \beta_\phi = -\beta_\omega \tan \epsilon / \tan(\theta_0 + \epsilon), \quad (8)$$

from which the strange couplings can be obtained as [7]

$$\beta_\omega^s / \beta_\omega = \alpha_\omega^s / \alpha_\omega = -\sqrt{6} \sin \epsilon / \sin(\theta_0 + \epsilon), \\ \beta_\phi^s / \beta_\phi = \alpha_\phi^s / \alpha_\phi = -\sqrt{6} \cos \epsilon / \cos(\theta_0 + \epsilon). \quad (9)$$

with  $\tan \theta_0 = 1/\sqrt{2}$ . The mixing angle  $\epsilon$  can be determined either from the radiative decays of the  $\omega$  and  $\phi$  mesons [12, 13, 14] or from their strong decays [15]. The value used here is  $\epsilon = 0.053$  rad ( $3.0^\circ$ ) [12].

Finally, the contributions of the up and down quarks to the electromagnetic form factors can be obtained from

$$G_{E/M}^u = 2G_{E/M}^p + G_{E/M}^n + G_{E/M}^s, \\ G_{E/M}^d = G_{E/M}^p + 2G_{E/M}^n + G_{E/M}^s. \quad (10)$$

### 4 Results

In order to calculate the nucleon form factors in the two-component model the five coefficients,  $\gamma$  from the intrinsic form factor,  $\beta_\omega$  and  $\alpha_\phi$  from the isoscalar couplings, and  $\beta_\rho$  and  $\alpha_\rho$  from the isovector couplings, are determined in a least-square fit to the electric and magnetic form factors of the proton and the neutron using the same data set as in [6]. The electromagnetic form factor of the proton and neutron are found to be in good agreement with experimental data [16]. According to Eq. (9), the strange couplings can be determined from the fitted values of the isoscalar couplings to be  $\beta_\phi^s = -\beta_\omega^s = 0.202$ ,  $\alpha_\phi^s = 0.648$  and  $\alpha_\omega^s = -0.018$  [16,17].

Figure 1 shows the strange Dirac and Pauli form factors as a function of the momentum transfer  $Q^2$ . Whereas the Pauli form factor is dominated by the coupling to the  $\phi$  meson ( $\alpha_\phi^s \gg \alpha_\omega^s$ ), the Dirac form factor is small due to a cancelation between the contributions from the  $\omega$  and  $\phi$  mesons ( $\beta_\phi^s = -\beta_\omega^s$ ). The qualitative features of these form factors can be understood in the limit of ideally mixed mesons, *i.e.* zero mixing angle  $\epsilon = 0$  (in comparison to the value of  $\epsilon = 3.0^\circ$  used in Figure 1). Since in this case

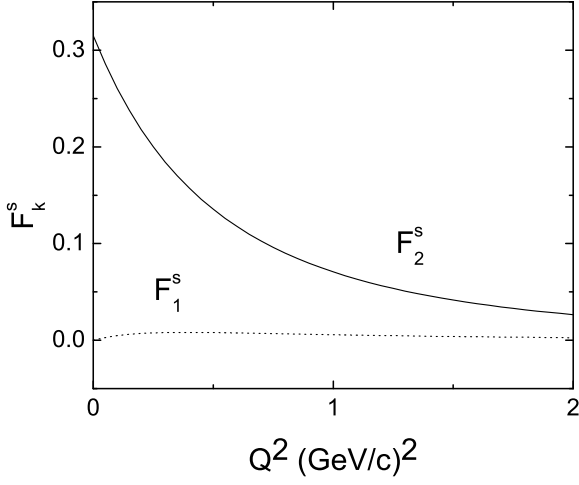


**Fig. 1.** Strange Dirac and Pauli form factors,  $F_1^s$  (dotted line) and  $F_2^s$  (solid line).

$\beta_\phi^s = \beta_\omega^s = \alpha_\omega^s = 0$ , the Dirac form factor vanishes identically and the Pauli form factor depends only on the tensor coupling to the  $\phi$  meson,  $\alpha_\phi^s$ .

The behavior of  $F_1^s$  and  $F_2^s$  in Figure 1 is quite different from that obtained in other theoretical approaches, especially for the strange Pauli form factor. Almost all calculations give negative values for  $F_2^s$  for the same range of  $Q^2$  values [7, 18, 19, 20, 21, 22], with the exception of the meson-exchange model [23] and the  $SU(3)$  chiral quark-soliton model [24]. In the former case, the values of  $F_2^s$  are about two orders of magnitude smaller than the present ones, whereas in the latter  $F_2^s$  is positive for small values of  $Q^2$ , but changes sign around  $Q^2 = 0.1 - 0.3$  (GeV/c) $^2$ .

Figures 2 and 3 show the strange electric and magnetic form factors as a function of  $Q^2$ . The theoretical values for  $G_E^s$  are small and negative, in agreement with the experimental results of the HAPPEX Collaboration in which  $G_E^s$  was determined in parity-violating electron scattering from  $^4\text{He}$ . The experimental values,  $G_E^s = -0.038 \pm 0.042 \pm 0.010$  measured at  $Q^2 = 0.091$  (GeV/c) $^2$  [25] and, more recently,  $G_E^s = -0.002 \pm 0.017$  at  $Q^2 = 0.1$  (GeV/c) $^2$  [27] are consistent with zero.

The values of  $G_M^s$  are positive, since they are dominated by the contribution from the Pauli form factor. Experimental evidence from the SAMPLE and HAPPEX collaborations gives a positive value of the strange magnetic form factor at  $Q^2 = 0.1$  (GeV/c) $^2$  of  $G_M^s = 0.37 \pm 0.20 \pm 0.26 \pm 0.07$  [28] and  $G_M^s = 0.12 \pm 0.24$  [27], respectively. The other experimental values of  $G_E^s$  and  $G_M^s$  in Figs. 2 and 3 for  $0.4 < Q^2 < 1.0$  (GeV/c) $^2$  were obtained [26, 29] by combining the (anti)neutrino data from E734 [30] with the parity-violating asymmetries from HAPPEX [31] and G0 [32]. The theoretical values are in good overall agreement with the experimental ones for the entire range  $0 < Q^2 < 1$  (GeV/c) $^2$ .

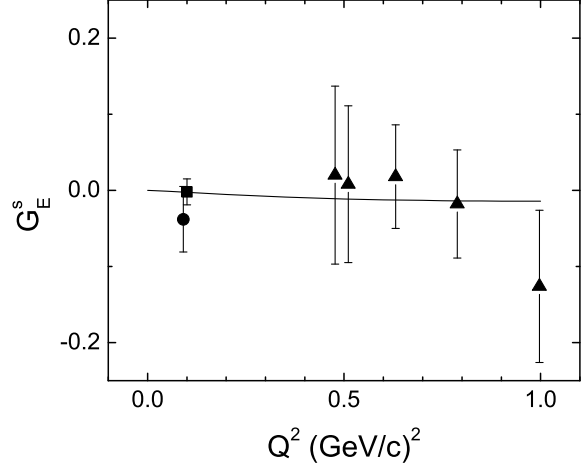


**Fig. 2.** Comparison between theoretical and experimental values of the strange electric form factor. The experimental values are taken from [25] (circle), [26] (triangle) and [27] (square).

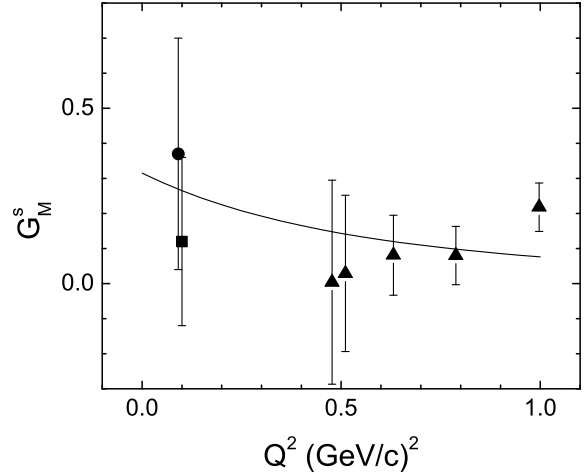


**Fig. 3.** Comparison between theoretical and experimental values of the strange magnetic form factor. The experimental values are taken from [28] (circle), [26] (triangle) and [27] (square).

**Table 1.** Comparison between theoretical and experimental values of strange form factors  $G_E^s + \eta G_M^s$ .

$Q^2$ (GeV/c) $^2$	$\eta$	$G_E^s + \eta G_M^s$		
		Present	Experiment	Reference
0.099	0.080	0.019	$0.030 \pm 0.028$	[4]
0.108	0.106	0.025	$0.071 \pm 0.036$	[33]
0.230	0.225	0.042	$0.039 \pm 0.034$	[34]
0.477	0.392	0.047	$0.014 \pm 0.022$	[31]

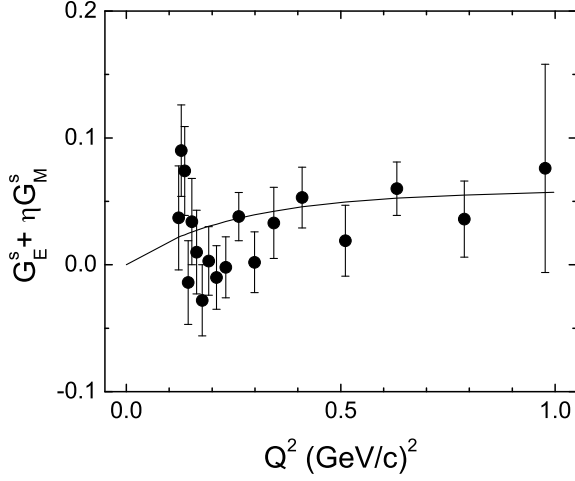


**Fig. 4.** Comparison between theoretical and experimental values of strange form factors  $G_E^s + \eta G_M^s$ . The experimental values were measured by the G0 Collaboration [32].

Table 1 and Figure 4 show the results obtained by the PVA4, HAPPEX and G0 collaborations for a linear combination of the strange electric and magnetic form factors  $G_E^s + \eta G_M^s$ . Also in this case, there is a good agreement between the calculated values and the experimental data.

In the majority of theoretical analyses, the strangeness contribution to the nucleon is discussed in terms of the static properties, the strange magnetic moment  $\mu_s$  and the strangeness radius  $\langle r_s^2 \rangle$ . Most theoretical studies agree on a small negative strangeness radius and a moderate negative strange magnetic moment [5], whereas the results of a combined fit of the strange electric and magnetic form factors measured by SAMPLE, PVA4 and HAPPEX at  $Q^2 \sim 0.1$  (GeV/c)<sup>2</sup>,  $G_M^s(0.1) = 0.55 \pm 0.28$  and  $G_E^s(0.1) = -0.01 \pm 0.03$  [4], indicate the opposite sign for both  $\mu_s$  and  $\langle r_s^2 \rangle$ . Recent lattice calculations give small negative values of the strange magnetic moment  $\mu_s = G_M^s(0) = -0.046 \pm 0.019 \mu_N$  [35] and the strange electric form factor  $G_E^s(0.1) = -0.009 \pm 0.028$  [36].

Figures 5 and 6 show the flavor decomposition of the electric and magnetic form factors of the proton. Note, that in comparison with Figs. 2 and 3 the flavor form factors have been multiplied by the quark electric charges, so that their sum gives the total form factor. The contribution of the strange quarks to the proton form factors is small for the entire range of  $Q^2$  values and of the order of a few percent of the total.

In the present approach, the strangeness contribution to the magnetic moment and the charge and magnetic radii is given by [17]

$$\mu_s = \frac{1}{2}(\alpha_\omega^s + \alpha_\phi^s) = 0.315 \mu_N,$$

$$\langle r_s^2 \rangle_E = 3\beta_\phi^s \left( \frac{1}{m_\phi^2} - \frac{1}{m_\omega^2} \right) + \frac{3}{4M_N^2}(\alpha_\omega^s + \alpha_\phi^s)$$

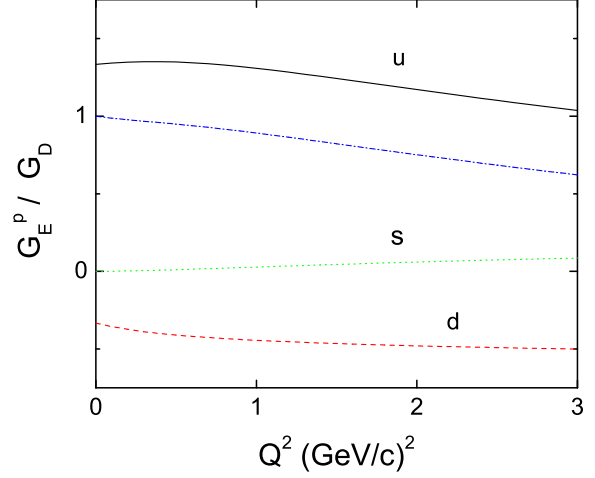


**Fig. 5.** Flavor decomposition of the proton electric form factor  $G_E^p / G_D$  with  $G_D = 1/(1 + Q^2/0.71)^2$ .

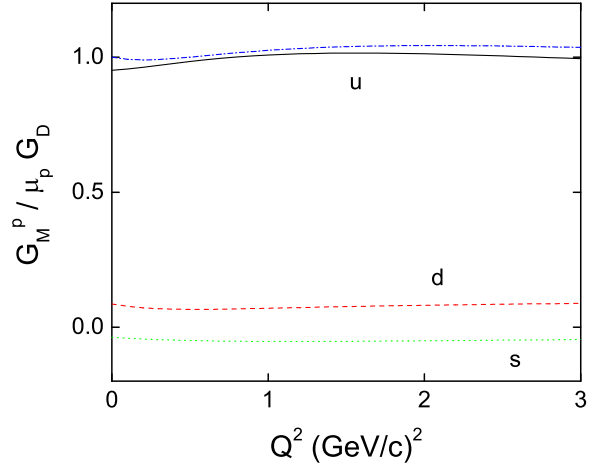


**Fig. 6.** Flavor decomposition of the proton magnetic form factor  $G_M^p / \mu_p G_D$  with  $G_D = 1/(1 + Q^2/0.71)^2$ .

$$= 0.005 \text{ fm}^2,$$

$$\langle r_s^2 \rangle_M = 6 \left[ 2\gamma + \frac{\beta_\phi^s + \alpha_\phi^s}{\alpha_\omega^s + \alpha_\phi^s} \frac{1}{m_\phi^2} + \frac{\beta_\omega^s + \alpha_\omega^s}{\alpha_\omega^s + \alpha_\phi^s} \frac{1}{m_\omega^2} \right]$$

$$= 0.410 \text{ fm}^2. \quad (11)$$

The strange magnetic moment does not depend on the mixing angle  $\epsilon$  [17] and its sign is determined by the sign of the tensor coupling  $\alpha_\phi^s$  ( $\gg \alpha_\omega^s$ ). The sign of the strangeness contribution to the magnetic moment and the charge radius is in agreement with the available experimental data. A positive value of the strange magnetic moment seems to preclude an interpretation in terms of

a  $uuds\bar{s}$  fluctuation into a  $AK$  configuration [37]. On the other hand, an analysis of the magnetic moment of  $uuds\bar{s}$  pentaquark configurations belonging to the antidecuplet gives a positive strangeness contribution for states with angular momentum and parity  $J^P = 1/2^+, 1/2^-$ , and negative for  $3/2^+$  states [38].

## 5 Summary and conclusions

In this contribution, the flavor content of nucleon form factors was studied in a VMD approach in which the two-component model of Bijker and Iachello for the electromagnetic nucleon form factors [6] is combined with the method proposed by Jaffe to determine the strangeness content via the coupling of the strange current to the  $\phi$  and  $\omega$  mesons [7]. The strange couplings are completely fixed by the electromagnetic form factors of the proton and neutron.

The good overall agreement between the theoretical and experimental values for the electromagnetic form factors of the nucleon and their strange quark content shows that the two-component model provides a simultaneous and consistent description of the electromagnetic and weak vector form factors of the nucleon. It was shown, that the strangeness contribution to the charge and magnetization distributions is of the order of a few percent. In particular, the strange magnetic moment is found to be positive, in contrast with most theoretical studies, but in agreement with the presently available experimental information from parity-violating electron scattering experiments.

Future experiments on parity-violating electron scattering to backward angles and neutrino scattering will make it possible to determine the contributions of the different quark flavors to the electric, magnetic and axial form factors, and thus to provide new insight into the complex internal structure of the nucleon.

## Acknowledgments

This work was supported in part by a research grant from CONACYT, Mexico.

## References

1. D.B. Kaplan and A. Manohar, Nucl. Phys. B **310**, 527 (1988); R.D. McKeown, Phys. Lett. B **219**, 140 (1989); D.H. Beck, Phys. Rev. D **39**, 3248 (1989).
2. D.H. Beck and R.D. McKeown, Annu. Rev. Nucl. Part. Sci. **51**, 189 (2001).
3. E.J. Beise, M.L. Pitt and D.T. Spayde, Prog. Part. Nucl. Phys. **54**, 289 (2005).
4. K.A. Aniol *et al.*, Phys. Lett. B **635**, 275 (2006).
5. D.H. Beck and B.R. Holstein, Int. J. Mod. Phys. E **10**, 1 (2001).
6. R. Bijker and F. Iachello, Phys. Rev. C **69**, 068201 (2004).
7. R.L. Jaffe, Phys. Lett. B **229**, 275 (1989).
8. F. Iachello, A.D. Jackson and A. Lande, Phys. Lett. B **43**, 191 (1973).
9. M.R. Frank, B.K. Jennings and G.A. Miller, Phys. Rev. C **54**, 920 (1996); E. Pace, G. Salmè, F. Cardarelli and S. Simula, Nucl. Phys. A **666**, 33c (2000).
10. R. Bijker, F. Iachello and A. Leviatan, Ann. Phys. (N.Y.) **236**, 69 (1994); Phys. Rev. C **54**, 1935 (1996).
11. G.P. Lepage and S.J. Brodsky, Phys. Rev. Lett. **43**, 545 (1979); Phys. Rev. D **22**, 2157 (1980).
12. P. Jain, R. Johnson, U.-G. Meissner, N.W. Park and J. Schechter, Phys. Rev. D **37**, 3252 (1988).
13. F. Iachello and D. Kusnezov, Phys. Rev. D **45**, 4156 (1992).
14. M. Harada and J. Schechter, Phys. Rev. D **54**, 3394 (1996).
15. C. Gobbi, F. Iachello and D. Kusnezov, Phys. Rev. D **50**, 2048 (1994).
16. R. Bijker, arXiv:nucl-th/0511004.
17. R. Bijker, J. Phys. G: Nucl. Part. Phys. **32**, L49 (2006) [arXiv:nucl-th/0511060].
18. N.W. Park and H. Weigel, Nucl. Phys. A **541**, 453 (1992).
19. G.T. Garvey, W.C. Louis and D.H. White, Phys. Rev. C **48**, 761 (1993).
20. H. Forkel, M. Nielsen, X. Jin and T.D. Cohen, Phys. Rev. C **50**, 3108 (1994).
21. H.-W. Hammer, U.-G. Meissner and D. Drechsel, Phys. Lett. B **367**, 323 (1996).
22. V.E. Lyubovitskij, P. Wang, Th. Gutsche and A. Faessler, Phys. Rev. C **66**, 055204 (2002).
23. U.-G. Meissner, V. Mull, J. Speth and J.W. Van Orden, Phys. Lett. B **408**, 381 (1997).
24. A. Silva, H.-Ch. Kim and K. Goeke, Eur. Phys. J. A **22**, 481 (2004).
25. K.A. Aniol *et al.*, Phys. Rev. Lett. **96**, 022003 (2006).
26. S.F. Pate, G. MacLachlan, D. McKee and V. Papavassiliou, arXiv:hep-ex/0512032.
27. K. Paschke, D.S. Armstrong, K. De Jager *et al.*, HAPPEX 2 Collaboration (2006), private communication.
28. D.T. Spayde *et al.*, Phys. Lett. B **583**, 79 (2004).
29. S.F. Pate, Phys. Rev. Lett. **92**, 082002 (2004).
30. L.A. Ahrens *et al.*, Phys. Rev. D **35**, 785 (1987).
31. K.A. Aniol *et al.*, Phys. Rev. C **69**, 065501 (2004).
32. D.S. Armstrong *et al.*, Phys. Rev. Lett. **95**, 092001 (2005).
33. F.E. Maas *et al.*, Phys. Rev. Lett. **94**, 152001 (2005).
34. F.E. Maas *et al.*, Phys. Rev. Lett. **93**, 022002 (2004).
35. D.B. Leinweber, S. Boinepalli, I.C. Cloet, A.W. Thomas, A.G. Williams, R.D. Young, J.M. Zanotti and J.B. Zhang, Phys. Rev. Lett. **94**, 212001 (2005).
36. D.B. Leinweber, S. Boinepalli, A.W. Thomas, P. Wang, A.G. Williams, R.D. Young, J.M. Zanotti and J.B. Zhang, arXiv:hep-lat/0601025.
37. B.S. Zou and D.O. Riska, Phys. Rev. Lett. **95**, 072001 (2005).
38. R. Bijker, M.M. Giannini and E. Santopinto, Phys. Lett. B **595**, 260 (2004).

